

Infrared, Laser-Raman and X-Ray Diffraction Investigation of MoO₃/ZrO₂ and the Oxidation of (Z)-But-2-ene

Hisashi Miyata,* Shoji Tokuda and Takehiko Ono*

Department of Applied Chemistry, University of Osaka Prefecture, Sakai, Osaka 591, Japan

Takashi Ohno and Fumikazu Hatayama

School of Allied Medical Sciences, Kobe University, Suma, Kobe 654-01, Japan

Molybdenum oxide supported on zirconia has been studied by XRD, FTIR and laser-Raman spectroscopy, together with the oxidation of (Z)-but-2-ene. Mo–Zr catalysts with less than 11 wt % of Mo loadings are mainly composed of amorphous polymolybdates. Mo–Zr catalysts with high MoO₃ loading exhibit high selectivities to acetaldehyde and acetic acid and both Lewis- and Brønsted-acidic sites by pyridine adsorption. On the other hand, the catalysts with low MoO₃ loading exhibit selectivities to furan and buta-1,3-diene and only Lewis sites. *In situ* FTIR and Raman spectra show the different character of Mo oxides with MoO₃ loading. This difference of Mo character leads to the difference in selectivities for butene oxidation.

Previously we have reported that the support effect observed with MoO₃ and V₂O₅ on TiO₂ and on ZrO₂,^{1–4} in the oxidation of alcohol and alkenes. In each case, polymolybdate or polyvanadate species were formed on these supports at low contents, their distorted structures bringing about the weakening of the Mo=O or V=O bond, and enhancement of the activity for the oxidation reactions. Such polymolybdate species are formed on Al₂O₃ or TiO₂.^{5–9} As regards Mo–Zr oxide catalysts, only a few papers have reported details of oxidation reactions. Furthermore, we have also reported that the acid–base properties of Mo–Ti¹⁰ and V–Zr¹¹ oxides change with the Mo or V content. Especially, in the V–Zr system, we proposed the reaction mechanism where Brønsted-acidic sites are important role in the oxidation of butene.¹¹

In this work, the structure of Mo–Zr oxide catalysts has been investigated by XRD, FTIR and laser-Raman techniques. The correlations between the surface structures of Mo oxides and the activity for butene oxidation have been discussed.

Experimental

The zirconium hydroxide was prepared from zirconium oxydichloride. The hydroxide was calcined at 383 K, followed by decomposition at 723 K. Catalysts were prepared by an impregnation method with a solution of ammonium heptamolybdate (MOZ3.0, MOZ7.5 and MOZ11.0, 3.0–11.0 wt % molybdenum oxide as MoO₃). MoO₃ was prepared by heating ammonium heptamolybdate at 723 K. The details of the preparation and pretreatments of the catalysts have been described previously.^{2,10} The physical parameters of these catalysts are listed in table 1.

Two types of apparatus were used. The first was a conventional closed-circulation system equipped with an IR cell in the circulation loop. The second was a pulse microreactor

system directly connected with a gas chromatograph for analysis of the reaction products. Details of the apparatus and procedures have been described in previous papers.^{2,12}

X-Ray diffraction patterns (XRD) of the catalysts were obtained on Rigaku Denki RAD-rA diffractometer using Cu K α radiation. The goniometer motor system and the signal were interfaced with a versatile data-acquisition system. As has been reported previously,^{1,2} a small amount of crystalline MoO₃ is detected by using a step-scanning method. The characterization of the Mo–Zr oxide structures was carried out using XRD, FTIR and laser-Raman techniques. The details of the data-acquisition and analysis system have been described previously.^{13–15}

For a pulse microreactor study, the dried catalysts were tested in a fixed-bed reactor. The catalyst charge of 30 mg was preheated with flowing oxygen for 1 h at 673 K, followed by flowing helium for 1 h at a reaction temperature of 473–673 K. Following pretreatment, a gaseous mixture of (Z)-but-2-ene, oxygen and helium (0.04 : 0.08 : 1.70 mmol) was fed over the catalyst. The reaction products were analysed by gas chromatography.

Results and Discussion

Microcatalytic Results

Oxidation of (Z)-but-2-ene was examined in the temperature range 473–673 K. As shown in fig. 1, the conversion of (Z)-but-2-ene increases with increasing MoO₃ loading as well as reaction temperature, and reaches saturated value at MoO₃ loading > 7.5 wt %. This suggests that the number of active sites is almost constant above 7.5 wt %. Reaction products varied with the reaction temperature and with MoO₃ loadings of catalysts. Fig. 2 shows the product selectivities of butene oxidation at various temperatures. The MOZ3.0 catalyst shows high selectivities to furan and buta-1,3-diene [fig. 2 (a), (b)]. These selectivities are higher at lower temperatures. On the other hand, the catalysts at high MoO₃ loadings show high selectivities to acetaldehyde and acetic acid. A small amount of butan-2-one was formed at low temperatures on both MOZ7.5 and MOZ11.0. At higher reaction temperatures, total oxidation to form CO and CO₂ took place significantly. The activities on Mo–Zr catalysts were ca. 5 times smaller than those on V–Zr oxides.⁴ Both pure ZrO₂ and MoO₃ showed little activity for the oxidation of (Z)-but-2-ene at these temperatures.

Table 1. Physical properties of Mo–Zr catalyst

catalyst	MoO ₃ (wt %)	surface area/m ² g ⁻¹	fraction of amorphous MoO ₃ (%)	surface conc. of amorphous oxide/ $\mu\text{mol mol}^{-2}$
MOZ3.0	3.0	49	100	4.2
MOZ7.5	7.5	46	89	10.0
MOZ11	11.0	39	76	15.0

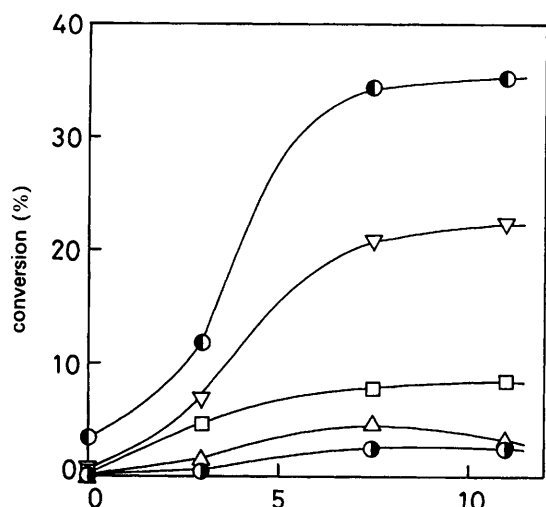


Fig. 1. Total conversion of (Z)-but-2-ene on Mo-Zr catalysts: ●, 473; △, 523; □, 573; ▽, 623; ○, 673 K.

FTIR Spectra of (Z)-but-2-ene on Mo-Zr Catalysts

As described above, Mo-Zr catalysts with MoO₃ loading > 7.5 wt % showed the same reactivities but different selectivities as compared with low MoO₃ loading catalyst. Therefore, we focused on the catalysts MOZ3.0 and MOZ7.5.

Fig. 3 shows the spectra of (Z)-but-2-ene adsorbed on MOZ7.5. When the MOZ7.5 catalyst is exposed to (Z)-but-2-ene at room temperature, the spectrum exhibits an OH band around 3660 cm⁻¹, CH stretching bands near 3000 cm⁻¹ and bands in the bending region. The spectrum below 2000 cm⁻¹ is seen after subtraction of catalyst itself. Sharp bands at 1462 and 1384 cm⁻¹ are due to the bending mode of CH₃ group of adsorbed butene. Considering that the band due to the π-complex on V-Ti oxide⁴ and on V-P oxides¹⁶ is observed at 1645 and 1625 cm⁻¹, respectively, a broad band at 1613 cm⁻¹ is assigned to stretching mode of C=C of π-bonded butene. The CH stretching bands at 2975 and 2925 cm⁻¹ are also in agreement with those of previous results.^{4,16} The ole-

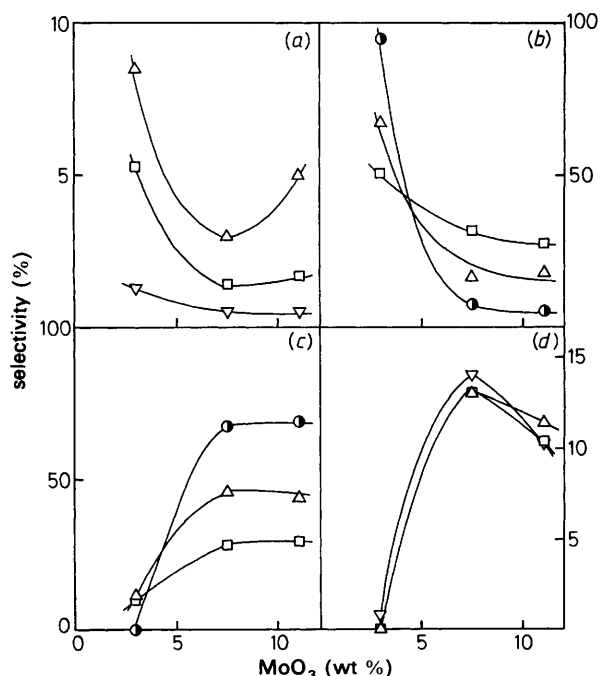


Fig. 2. Products selectivity of (Z)-but-2-ene oxidation on Mo-Zr catalysts: (a) furan, (b) buta-1,3-diene, (c) CH₃CHO, (d) CH₃COOH; ●, 473 K; △, 523 K; □, 573 K; ▽, 623 K.

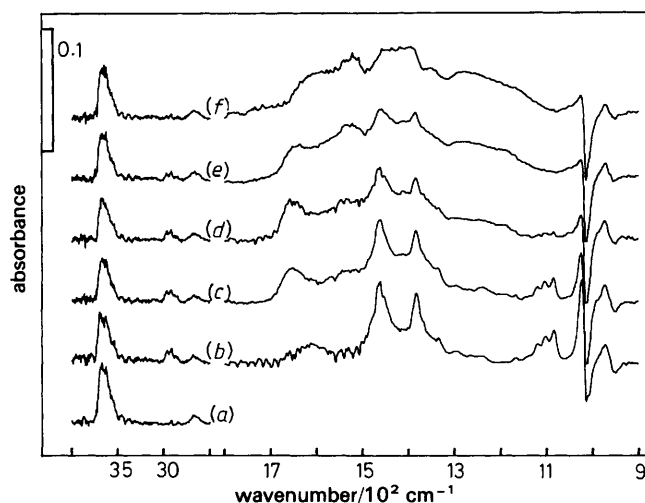


Fig. 3. FTIR spectra of (Z)-but-2-ene adsorbed on MOZ7.5. (a) Background, (b) after introduction of (Z)-but-2-ene (ca. 1.1 kPa for 30 min at 293 K), (c) followed by 30 min at 323 K in oxygen, (d) 30 min at 353 K in oxygen, (e) 30 min at 383 K; (f) 30 min at 443 K in oxygen. The spectra of (b)-(f) below 1800 cm⁻¹ show after subtraction of background.

finic CH bands above 3000 cm⁻¹ could not be detected in the spectra. Thus, it may be concluded that (Z)-but-2-ene is adsorbed as a π-complex on MOZ7.5 at room temperature. In addition, bands appeared at 1119, 1100 and 1084 cm⁻¹, in agreement with those of surface butoxide species (not shown in the figure). This implies the formation of C—O bonds as well as π-complexes from butene at low temperature. Considering that the spectrum has the catalyst spectrum subtracted from it, a negative band at 1000 cm⁻¹, which is due to the Mo=O species in the catalyst as will be discussed below, suggests that the adsorbed species interact with surface Mo=O in the catalyst and the Mo=O band reduced in intensity.

Oxygen (2.7 kPa) was admitted to the MOZ7.5 containing (Z)-but-2-ene, and the temperature of the catalyst was raised in stages under circulation of oxygen. With increasing disc temperature the intensities of the bands due to the π-complex and alkoxide species decreased, and simultaneously a new band appeared at 1656 cm⁻¹ at 323 K [fig. 3(c)]. This is assigned to the C=O stretching vibration of coordinated ketones on surface Lewis-acidic sites. Furthermore, a new band at 1538 cm⁻¹ was observed at 383 K; this is considered to be from an enol-type species, which is dehydrogenated from ketones [fig. 3(d)].⁴ The bands due to surface acetate and formate species were found at higher temperature [fig. 3(e)].

Similar experiments were carried out with MOZ3.0 (fig. 4). Only weak bands of adsorbed (Z)-but-2-ene were observed at almost the same positions as those in the MOZ7.5 at room temperature, but the bands due to alkoxide species were not found [fig. 4(b)]. The temperature of the catalyst was raised in stages under circulation of oxygen. At 383 K new bands, which were not observed with MOZ7.5, appeared at 1666, 1613 and 1392 cm⁻¹ [fig. 4(e)]. Similar bands were observed on the V-Zr catalysts with monolayer vanadia, and were attributed to a dihydrofuran-like species.⁴ The bands due to ketones or enol-type species were not observed. As same as with MOZ7.5, acetate and formate species were found at higher temperature.

Adsorption of Pyridine on Mo-Zr Oxides

The above results show that Mo-Zr oxide catalysts with high MoO₃ loadings favour the formation of oxygen-containing

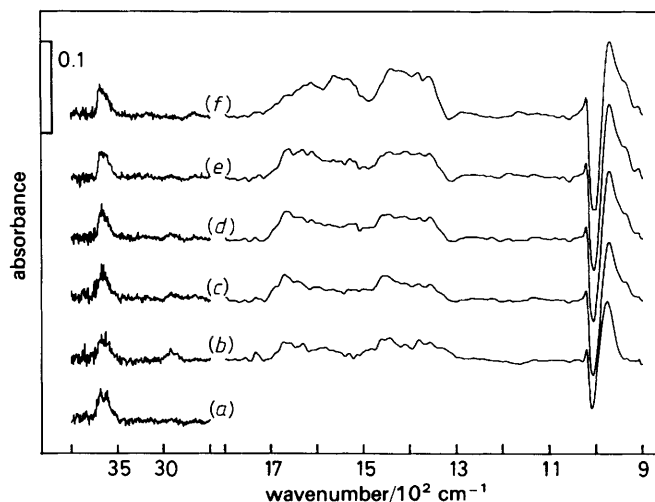


Fig. 4. FTIR spectra of (Z)-but-2-ene adsorbed on MOZ3.0. (a) Background, (b) after introduction of (Z)-but-2-ene (ca. 1.1 kPa for 30 min at 293 K), (c) followed by 30 min at 323 K in oxygen, (d) 30 min at 353 K in oxygen, (e) 30 min at 383 K in oxygen, (f) 30 min at 443 K in oxygen. The spectra of (b)–(f) below 1800 cm^{-1} show after subtraction of background.

intermediates and the cleavage of C–C bonds. This reaction is considered to proceed according to the oxyhydrative scission mechanism, which is closely related to the surface Brønsted acidity.¹⁷ Therefore, we examined the adsorption of pyridine to clarify the surface acidity of Mo–Zr oxides.

The use of pyridine as a selective probe molecule to characterize both qualitative and quantitative aspects of surface acidity is widespread. The assignments of the IR bands are in agreement with the well established correlation between the band positions and the type of interaction between pyridine and the site on which it is adsorbed.

As shown in fig. 5, admitting pyridine to MOZ7.5 at room temperature led to the appearance of sharp bands at 1609, 1489 and 1450 cm^{-1} together with weak bands at 1639, 1578 and 1540 cm^{-1} [fig. 5(b)]. From a comparison of the IR spectra of pyridine adsorbed on various metal oxides,^{10,11,18} the bands at 1609, 1578, 1489 and 1450 cm^{-1} are characteristic of Lewis-coordinated pyridine (LPy), and the bands at

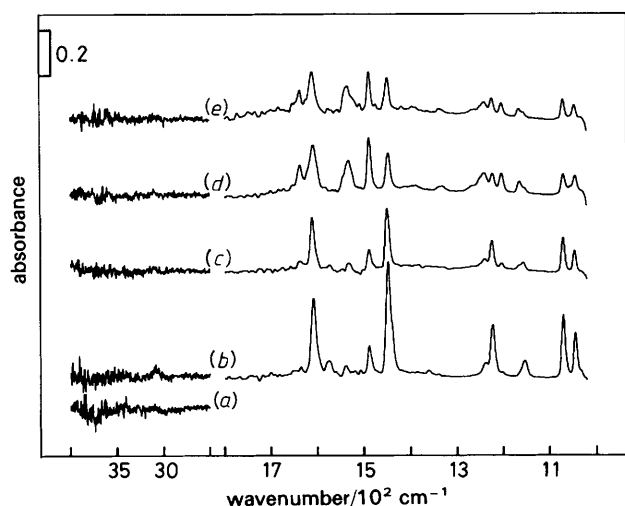


Fig. 5. FTIR spectra of pyridine adsorbed on MOZ7.5. (a) Background, (b) introduction of a small amount of pyridine followed by 30 min evacuation at 293 K, (c) followed by 30 min evacuation at 373 K, (d) followed by introduction of water vapour at 293 K, (e) followed by 30 min evacuation at 373 K. The spectra of (b)–(e) below 1800 cm^{-1} show after subtraction of background.

1639, 1578, 1540 and 1489 cm^{-1} are characteristic of pyridinium ion (BPy). The intensity of each band decreased upon evacuation at 373 K [fig. 5(c)]. Since it is expected that some water is present in the oxidation reaction, we examined the effect of water vapour on the surface acidity. The introduction of a small amount of water at room temperature to MOZ7.5 samples with preadsorbed pyridine caused the intensification of BPy bands and the corresponding reduction of LPy bands [fig. 5(d)], suggesting that any strong Lewis-acidic sites on MOZ7.5 react with water to form a Brønsted-acidic site. These bands remained almost unchanged at 373 K [fig. 5(e)]. The results led to the conclusion that on MOZ7.5 catalysts there exist both Lewis- and Brønsted-acidic sites, and Mo=O bond or Lewis-acidic sites can easily convert to Brønsted-acidic sites.

Similar experiments were carried out with MOZ3.0 catalysts (fig. 6). Admission of pyridine at room temperature led to the appearance of the LPy bands, but BPy bands were not observed [fig. 6(b)]. As in the case of MOZ7.5, a decrease in band intensity was observed upon evacuation at 373 K [fig. 6(c)]. The addition of a small amount of water caused no change in the spectral feature. Thus, it is concluded that the conversion from Lewis-acidic sites to Brønsted-acidic sites does not occur on the MOZ3.0 catalysts and that only Lewis-acidic sites exist on the MOZ3.0 catalysts in the reaction condition.

Structure Characterization of Mo–Zr Oxide Catalysts

XRD patterns of the catalysts showed that no diffraction lines were observed corresponding either to a new phase or to crystalline MoO₃ with MOZ3.0, while the diffraction lines due to crystalline MoO₃ were observed with MOZ7.5 and MOZ11.0. The crystallinity of the MoO₃ phase in the catalysts was determined from the average intensities with Mo–Zr oxides and the corresponding physical mixtures of pure MoO₃ and ZrO₂.² The concentrations of amorphous surface molybdate species per surface area are listed in table 1. Although the calculation of amorphous species from XRD lines may include some errors, the concentrations of these species increase with increasing molybdenum loadings. From the XRD data it follows that with MOZ3.0 ca. 100% of the molybdenum oxide is present as an amorphous phase, while

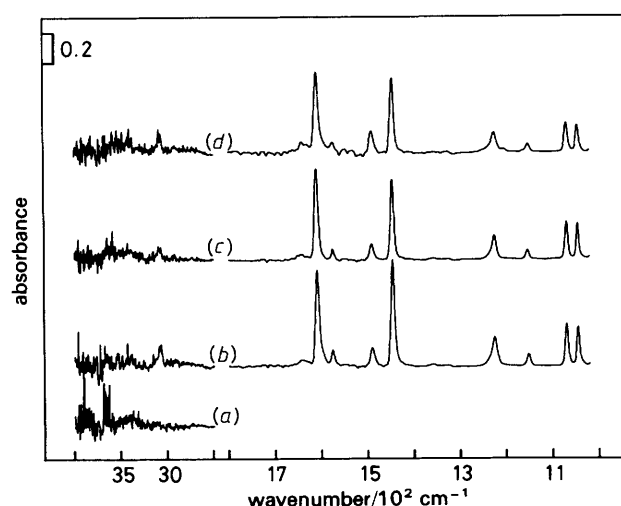


Fig. 6. FTIR spectra of pyridine adsorbed on MOZ3.0. (a) Background, (b) introduction of a small amount of pyridine followed by 30 min evacuation at 293 K, (c) followed by 30 min evacuation at 373 K, (d) followed by introduction of water vapour at 293 K. The spectra of (b)–(e) below 1800 cm^{-1} show after subtraction of background.

with MOZ7.5 and MOZ11.0 the percentages are 89 and 76%, respectively.

Fig. 7 shows the laser-Raman spectra of ZrO_2 support and of Mo-Zr oxide catalysts after subtraction of the background using spline functions. The spectra were obtained immediately after calcination at 673 K. With pure ZrO_2 , a number of bands were observed below 650 cm^{-1} . Mo-Zr oxides show the bands which are attributed to the stretching vibration of Mo=O in the region $950\text{--}1000\text{ cm}^{-1}$. It has been reported that crystalline phases are considerably more Raman active than amorphous phases.^{19,20} Similar results were observed with MOZ11.0, where ca. 24% of the Mo oxide is present as a crystalline phase as shown by XRD (table 1). Typical bands at 998 and 824 cm^{-1} due to crystalline MoO_3 are very strong. The bands due to amorphous phase were observed at 957 cm^{-1} with MOZ3.0, at 970 cm^{-1} with MOZ7.5 and at 980 cm^{-1} with MOZ11.0. The band positions are shifted to higher wavenumber with increasing MoO_3 loadings. These results are in agreement with the previous work.²

It has been reported that polyanions exhibit Raman bands at $940\text{--}950\text{ cm}^{-1}$; that MoO_4^{2-} has a band at 895 cm^{-1} ,²¹ and that octahedrally coordinated polymolybdates increase with increasing surface coverage or during calcination procedures.^{5,6,8} Thus, considering that in this study the Raman data were obtained after calcination at 673 K, the bands at $950\text{--}980\text{ cm}^{-1}$ are attributed to the stretching vibration of the terminal Mo=O bond of polymolybdate species on ZrO_2 .

In this work, the bands due to Mo=O stretching vibrations were shifted from 957 to 980 cm^{-1} on going from MOZ3.0 to MOZ11.0. Similar results have been reported with W-Al/Ti oxide and Mo-Al/Ti oxide.⁷ With the Raman data obtained in ambient air in this work, we can give the same explanation. In fact, *in situ* Raman spectra of MOZ7.5 (not shown in the figure) showed such a frequency shift, i.e. the band was obtained at almost the same position as crystalline MoO_3 after calcination in O_2 atmosphere, and shifted to lower wavenumber following H_2O exposure.²²

In the present study, the spectral behaviour in the Mo=O region on the adsorption of pyridine and on reaction with

butene was investigated by *in situ* IR spectroscopy. The zirconia support showed no absorption band in the region from $1100\text{--}900\text{ cm}^{-1}$. Thus, spectral behaviour in the Mo=O region on adsorption or evacuation could be observed in detail. The spectra below 1100 cm^{-1} corresponding to that in fig. 5 and 6 are shown in fig. 8. The Mo=O bands appeared at 997 cm^{-1} for MOZ3.0 and at 1003 cm^{-1} for MOZ7.5, respectively, after oxidation at 673 K [fig. 8(a)]. From the results of XRD and Raman studies, it is concluded that these bands are due to polymolybdates. For MOZ3.0, the introduction of pyridine caused a remarkable shift to lower wavenumber (975 cm^{-1}) and a reduction in intensity [fig. 8A(b)]. Furthermore, this band was shifted to slightly lower wavenumber (966 cm^{-1}) upon admission of H_2O at room temperature [fig. 8A(c)]. On the other hand, for MOZ7.5 the introduction of pyridine caused a complex band shape, as shown in fig. 8B(b). Following introduction of H_2O further modification of band shape occurred [fig. 8B(d)], although we observed little or no significant change in the OH region [fig. 5(d)]. Such a difference of spectral behaviour between MOZ3.0 and MOZ7.5 is interpreted to the difference of Mo=O bond character and of surface acidities. On MOZ7.5 the formation of surface OH groups, which act as Brønsted sites, is promoted by the introduction of H_2O , so the corresponding change of band shape is observed in fig. 8. On the other hand, H_2O molecules on MOZ3.0 coordinate to Mo=O bonds, but do not act as Brønsted sites. The Mo=O bands, which were observed in almost reaction conditions of butene oxidation are shown in fig. 3 and 4. The spectral behaviour in the Mo=O region depends on the Mo content in the catalyst.

Although the value of 7.5 wt % is estimated to be the MoO_3 content for which the theoretical monolayer is formed on the ZrO_2 support, it can easily be imagined that Mo oxides aggregate during the calcination procedure and form partial multilayers. Recently Machej *et al.*²³ have reported that the impregnation leads to a poor dispersion of molybdena on the surface of titania, which is due to the clustering of molybdena when the MoO_3 loading does not exceed the theoretical monolayer coverage. In fact, the spectrum of MOZ7.5 obtained after oxidation at 673 K already shows a

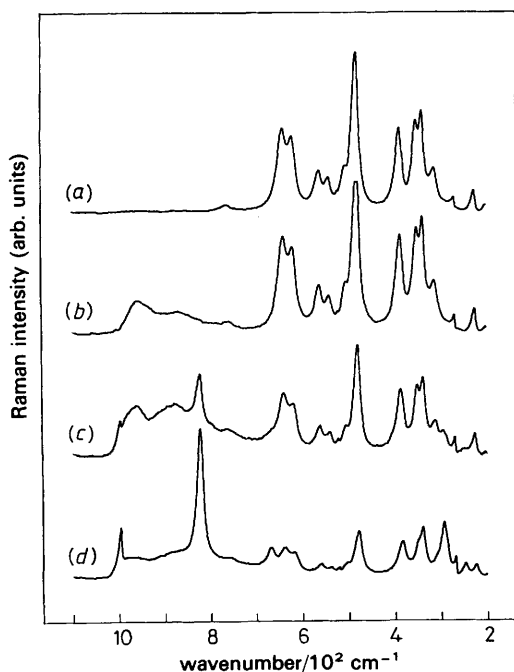


Fig. 7. Laser-Raman spectra of catalysts: (a) ZrO_2 , (b) MOZ3.0, (c) MOZ7.5, (d) MOZ11.0.

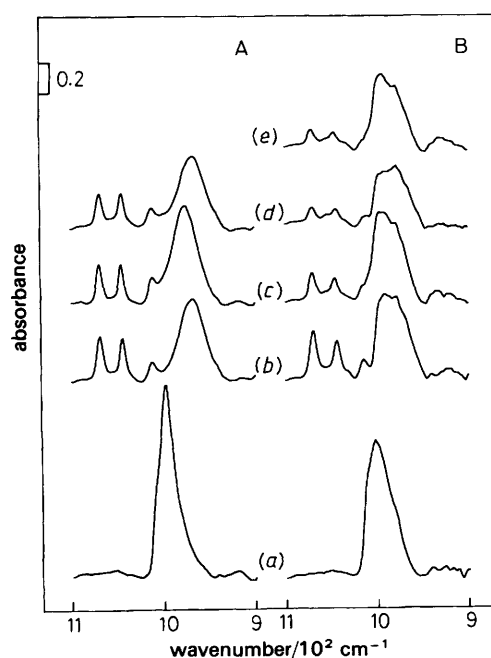


Fig. 8. FTIR spectra of pyridine adsorbed on catalysts: (A) MOZ3.0, (B) MOZ7.5. Symbols as for fig. 5 and 6.

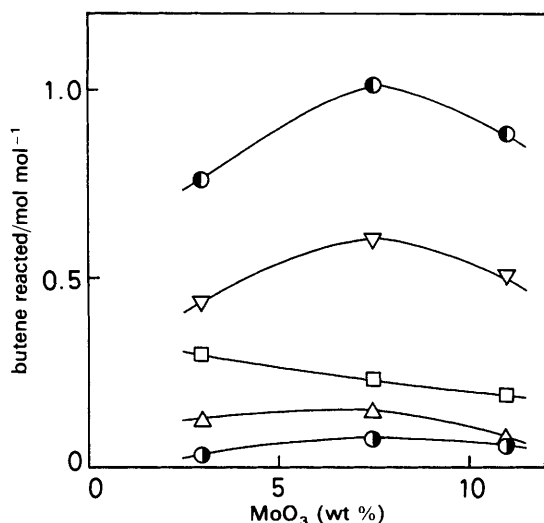


Fig. 9. Catalytic activities per amorphous Mo-oxide: ●, 473; △, 523; □, 573; ▽, 623; ●, 673 K.

more complex band shape [fig. 8B(a)]. As in the case of V-Zr oxide catalysts,¹¹ the Mo oxide in MOZ3.0, which corresponds to the monolayer catalyst in V-Zr systems, is expected to be uniformly dispersed on the catalyst surface, thus the Mo=O band seems to be composed of almost a single peak. On the other hand, the MOZ7.5, which corresponds to the multilayer catalyst in V-Zr systems, seems to contain two or more species of Mo oxide on the surface. However, further discussion will not be given in the present paper.

Structure, Surface Acidity and Catalytic Activities

From the above results we can conclude that polymolybdates formed on ZrO₂ are active sites for the oxidation of (*Z*)-but-2-ene. Fig. 9 shows the activity per amorphous molybdate, which is estimated from XRD. The amounts of butene reacted differ insignificantly on MOZ3.0 and MOZ7.5–11.0. However, the selectivities of the reaction differ with MoO₃ loadings. FTIR spectra also show that oxygen-containing intermediates are easily formed on MOZ7.5 catalysts, but not on MOZ3.0.

Raman and FTIR studies reveal the difference of structures and surface acidities between the MOZ3.0 and MOZ7.5. The MOZ7.5 has a high concentration of Brønsted-acidic sites. Thus, the oxyhydrative scission¹⁷ of the C—C bond is closely related to the Brønsted acidity on this catalyst. At low Mo loadings (MOZ3.0), the Mo=O species seems to be weaker and is affected by the presence of reactants and products under the oxidation reaction. The low MoO₃ loading catalyst

has few or no Brønsted sites, only Lewis sites. Thus, polymolybdate species at low Mo loadings seem to have some unsaturated coordination sites, which easily lead to the dehydration of butenes. The weakening of the Mo=O bond by the presence of compounds seems to be closely related to the enhancement of dehydrogenation. From the above considerations, a situation similar to that reported for the V-Ti³ and V-Zr¹¹ systems is expected in this work.

References

- 1 T. Ono, Y. Nakagawa, H. Miyata and Y. Kubokawa, *Bull. Chem. Soc. Jpn*, 1984, **57**, 1205.
- 2 T. Ono, H. Miyata and Y. Kubokawa, *J. Chem. Soc., Faraday Trans. 1*, 1987, **83**, 1761.
- 3 T. Ono, T. Mukai, H. Miyata, T. Ohno and F. Hatayama, *Appl. Catal.*, 1989, **49**, 273.
- 4 H. Miyata, M. Kohno, T. Ono, T. Ohno and F. Hatayama, *J. Chem. Soc., Faraday Trans. 1*, 1989, **85**, 3663.
- 5 H. Jeziorowski and H. Knözinger, *J. Phys. Chem.*, 1979, **83**, 1166.
- 6 K. Y. S. Ng and E. Gulari, *J. Catal.*, 1985, **92**, 340.
- 7 S. S. Chan, I. E. Wachs, L. L. Murrell, L. Wang and W. K. Hall, *J. Phys. Chem.*, 1984, **88**, 5831.
- 8 H. Knözinger and H. Jeziorowski, *J. Phys. Chem.*, 1978, **82**, 2002.
- 9 J. M. Stencel, L. E. Makovski, T. A. Sarkus, J. D. Vries, R. Thomas and J. A. Moulijn, *J. Catal.*, 1984, **90**, 314.
- 10 H. Miyata, T. Mukai, T. Ono and Y. Kubokawa, *J. Chem. Soc., Faraday Trans. 1*, 1988, **84**, 4137.
- 11 H. Miyata, M. Kohno, T. Ono, T. Ohno and F. Hatayama, *Appl. Catal.*, submitted for publication.
- 12 H. Miyata, T. Mukai, T. Ono, T. Ohno and F. Hatayama, *J. Chem. Soc., Faraday Trans. 1*, 1988, **84**, 2465.
- 13 H. Miyata, K. Fujii, T. Ono, Y. Kubokawa, T. Ohno and F. Hatayama, *J. Chem. Soc., Faraday Trans. 1*, 1987, **83**, 675.
- 14 H. Miyata, K. Fujii, S. Inui and Y. Kubokawa, *Appl. Spectrosc.*, 1986, **40**, 1177.
- 15 H. Miyata, S. Tokuda and T. Yoshida, *Appl. Spectrosc.*, 1989, **43**, 522.
- 16 A. Ramstetter and M. Baerns, *J. Catal.*, 1988, **109**, 303.
- 17 T. Seiyama, K. Nita, T. Maehara, N. Yamazoe and Y. Takita, *J. Catal.*, 1977, **49**, 164; Y. Takita, K. Nita, T. Maehara, N. Yamazoe and T. Seiyama, *J. Catal.*, 1977, **52**, 364; Y. Takita, T. Maehara, N. Yamazoe and T. Seiyama, *J. Catal.*, 1987, **104**, 359.
- 18 H. Miyata, K. Fujii and T. Ono, *J. Chem. Soc., Faraday Trans. 1*, 1988, **84**, 3121.
- 19 F. Roozeboom, J. A. Medema and P. J. Gellings, *Z. Phys. Chem., NF* 1978, **111**, 215.
- 20 F. P. I. Kerkhof, J. A. Moulijn, R. Thomas and J. C. Oudejans, *Preparation of Catalysts II* (Elsevier, Amsterdam, 1979) p. 77.
- 21 W. P. Griffith and P. J. B. Lesniak, *J. Chem. Soc. A*, 1969, 1066.
- 22 H. Miyata, S. Tokuda and T. Ono, unpublished data.
- 23 T. Machej, B. Doumain, B. Yasse and B. Delmon, *J. Chem. Soc., Faraday Trans. 1*, 1988, **84**, 3905.